JOURNAL OF MATERIALS SCIENCE 31 (1996) 4865–4870

Numerical experiments on paper-fluid interaction – permeability of a three-dimensional anisotropic fibre network

D. QI*, T. UESAKA
Pulp and Paper Research Institute of Canada, 570 St. John's Boulevard, Pointe Claire Quebec, Canada, H9R 3J9

The effect of paper structure on flow characteristics of various fluids is one of the most important, fundamental problems in papermaking, coating, and printing. A computer code based on a cellular automaton model, in particular the lattice-gas Boltzmann model, has been developed to simulate flow numerically in a random fibre network. As a preliminary investigation, a numerical experiment has been conducted on the three-dimensional permeability of an interpenetrable fibre network. It was found that the in-plane permeability and the *z*-directional (thickness direction) permeability are very sensitive to the distribution of fibre segments in the *z*-direction. At a constant porosity, the *z*-directional permeability increases and the in-plane permeability decreases with increasing *z*-directional fibre orientation.

1. Introduction

Penetration, spreading and flow of fluids in a porous paper structure occur in almost all important processes of papermaking and in the end use. In wet pressing and drying processes, permeability of the wet web determines drainage resistance and drying efficiency [1, 2]. It is also well known that the drainage resistance affects the consolidation process of the sheet structure, determining non-uniformity of density in the thickness direction [3]. The penetration of coating colour into the sheet structure affects runnability of base stock on the coater, the coat structure, and thus final quality of coated paper. Ink spreading and penetration are other important examples of three-dimensional paper-fluid interactions controlling printability and print quality [4, 5].

Although considerable effort has been spent to understand the basic mechanism of paper structure-fluid interactions, many of the approaches are still phenomenological and are often of an empirical nature. This is because of the extreme difficulty in directly describing the complex random fibre network structure of paper. For example, the pore structure of paper is often represented by a group of cylindrical capillaries. The Hagen–Poiseuille equation is employed to relate the flow rate and the pressure drop. To take into account the effects of the complex pore structure, various structural parameters are introduced, such as porosity, tortuosity factor, shape factor, and hydrodynamic specific surface area. The Kozeny–Carman equation has been widely used to analyse results of permeability in terms of such structural parameters [6]. Relating these parameters to real paper structure, however, is not straightforward because of the empirical nature of the model. In addition, the treatment is essentially one-dimensional so that the problem of direction-dependent flow, such as in-plane spreading and penetration in the thickness direction, cannot be treated within the framework of the empirical model.

This paper describes an attempt to deal directly with the flow in the random fibre network structure without resorting to empirical models. The method is based on the cellular-automaton fluid model, in particular the lattice-gas Boltzmann model, which was originally introduced by Frisch *et al.* [7, 8]. As an illustrative example, permeability parameters in the three directions are computed for different degrees of fibre orientation in the thickness direction of paper (the *z*-direction). The main objectives of this paper are, first to demonstrate the potential of the lattice-gas Boltzmann method for numerically modelling fluid flow in an anisotropic three-dimensional fibre network, and secondly to acquire basic knowledge of the effects of the microstructure on paper permeability.

2. Background

Various approaches have been taken to predict quantitatively the permeability of random porous materials. Rigorous upper and lower bounds of permeability have been obtained by applying variational principles to the Stokes equation [9–13]. In the case of random anisotropic structures, such as paper sheets, this

Present address: Western Michigan University, Kalamazoo, MI, USA.

0022–2461

method requires anisotropic pair distribution functions to be obtained, which, at this moment, cannot easily be obtained by either analytical or numerical methods. Less rigorous methods are the electrical resistor analogue approaches [14, 15]. The pore structure is represented by the network of the conductance elements, and the conductance of each element is selected to represent flow characteristics of specific pore structures, such as the pore throat. The effective medium theory or Monte Carlo method has been used to calculate the overall conductance (or effective permeability). Because this approach avoids solving the Navier–Stokes equations directly, it is again difficult to relate the flow characteristics to real paper structure.

A direct approach to tackling this problem may be to use a finite element method or a finite difference method. The advantage of these methods is that there are a number of sophisticated commercial codes, including pre- and post-processors, available on the market. However, the grossly irregular, random structure of paper may limit the range of numerical simulation to an unrealistically small structural element, depending on the computer capacity.

The recent development of the cellular-automaton fluid models, and its extension to the three-dimensional lattice-gas Boltzmann model [16, 17], proposed by Chen et al. [18] in 1992, has provided a new computational scheme for fluid dynamics. This alternative numerical method is a powerful tool to solve accurately the Navier–Stokes equations for complex geometrical systems, particularly for random porous media. (Because the lattice-gas models are still in the early stage of the development, there is no direct comparison between the finite element/difference methods and the lattice-gas methods).

3. Cellular-automaton fluid models

In the cellular-automaton fluid models [8], we consider a lattice containing moving particles. The "artificial" particles randomly populate the lattice nodes and collide with each other according to a set of collision rules. The collision rules are derived so as to satisfy mass and momentum conservation at each node. (It should be noted that "particles" and their "movement" in the cellular-automaton models represent neither real molecules nor molecular motion, in contrast to molecular dynamics models, but the models essentially represent a "fictitious" micro-world). Using suitable restrictions of the crystallographic symmetry of the lattice and taking proper limits of micro-dynamical equations in time and space, one can show that the micro-dynamical equations are reduced to the incompressible Navier–Stokes equations (macro-dynamical equations) as a special case. In other words, one can simulate fluid dynamical phenomena by using the discrete lattice-gas model without directly solving the Navier–Stokes equations. In spite of the simple collision rules, the models can exhibit rich macroscopic complexity, such as turbulence. The simple microscopic rules have a special advantage, that is, the basic algorithm becomes very simple and is particularly suited for massively-parallel computing. Another advantage is that irregular boundary conditions can be easily handled. This feature is especially important in the simulation of fluid flow in random porous media.

The model used in this study is the lattice-gas Bolzmann model [17] using the face-centred hypercubic lattice to deal with the three-dimensional fluid [8, 16]. The general outline of the lattice-gas models can be found elsewhere [7, 19].

4. Numerical experiments

4.1. Simulation of flow in a pipe

Permeability is defined by the Darcy law

$$U = -\frac{K}{\rho\nu}\nabla P \tag{1}$$

where U is a velocity vector, K is a second-order permeability tensor, ν is the kinematic viscosity, ρ is the density of the fluid and P is pressure. If a Cartesian coordinate system is chosen to coincide with the principal directions of the fibre network, three principal components of the permeability tensor, K_x, K_y and K_z correspond to permeability in the machine direction, in the cross machine direction, and in the thickness direction, respectively. Darcy's law is valid only when the Reynolds number, Re, is small enough that the viscous force dominates the inertial force. Therefore, the flow rates used for the simulation should be limited to the range where Darcy's law holds [19]. (Recently, the case of higher Reynolds number has been successfully dealt with by this model [20].)

In order to check the validity of the simulation model and the Fortran code, we have applied this model to the well-known Poiseuille flow in a pipe where an analytical solution is available. The square cross-section of the pipe consists of 19×19 unit cells. In this simulation, all units are natural units, i.e. the units of time, mass, and length are taken as 1. The average particle density is 8.175, the kinematic viscosity is 0.15. No-slip boundary conditions are imposed, i.e. whenever particles hit the solid nodes, they are reflected back into the fluid along the opposite direction. The pressure gradient is created by increasing the populations of particles proportionally to the "body force" in the x-direction at each automaton step. Periodic boundary conditions are applied along the x-direction and no-slip boundary conditions are applied on the surface of the pipe. After about 1000 time steps, the system reached an equilibrium state, and the flow rate Q, was calculated from

$$Q = \int V \mathrm{d}y\mathrm{d}z \tag{2}$$

where V is the velocity of fluid, and the mean flow rate U can be obtained from $U = Q/H^2$, where H is the width of the pipe. Results were compared with the analytical solution of the Poisson equation with Dirichret boundary conditions at the pipe wall [21].

$$U = \frac{0.035H^2F}{\nu} \tag{3}$$

In this equation, F is the body force applied to create the pressure gradient. Table I shows comparisons of

TABLE I Comparisons between numerical results and analytical solutions obtained from Equation (natural unit)

Body force, F	Mean velocity (analytical)	Mean velocity (numerical)	Error (%)
0.001 1800	0.099 40	0.099 48	0.080 48
0.000 5090	0.042 87	0.042 91	0.093 31
0.000 2545	0.021 44	0.021 45	0.004 66

the numerical results with the analytical solutions for different values of the body force applied. Within the range tested, the mean velocity obtained from the simulation was proportional to the body force, as expected from the analytical solution, and the errors were within 0.1%.

4.2. Simulation of flow in a random fibre network

For the simulation of flow through the fibre network, it is necessary to have information about the three-dimensional fibre network structure. Currently, only limited quantitative data of paper structure are available in the literature [22]. Therefore, in this paper we will construct a configuration retaining the basic structural features of the fibre network, i.e. randomness and anisotropy. The model of "fully penetrable" cylinders with randomly placed axes has been employed by Tsai and Strieder [23] and Torquato and Beasley [24] in the studies of isotropic fibrous media. In this paper we modify their model to construct an anisotropic, fully penetrable fibre network. The procedure of constructing the fibre network is as follows. First, the simulation box of $100\,\mu m \times 100\,\mu m \times 100\,\mu m$ is divided into a lattice of $36 \times 36 \times 36$ with the unit length 2.7778 μm as shown in Fig. 1a. Then, the centre of a fibre with rectangular cross-section is randomly located at a node with the coordinates (x_0, y_0, z_0) shown in Fig. 1b. The fibre (the broken lines in Fig. 1b) initially lies in the plane parallel to the $x - y$ plane with the long side parallel to the x-axis. The fibre is then rotated through an angle ϕ around the z-axis, as indicated by the dashed line, subsequently rotated through a z-directional polar angle, θ. In this simulation, the angle ϕ is uniformly and randomly distributed between 0° and 180° to construct a fibre network isotropic in the $x - y$ plane, modelling handsheets. The polar angle, θ, is also assumed to be randomly and uniformly distributed between $\theta = -\omega$ and $\theta = +\omega$. All the fibres intersect the wall of a simulation box (no fibre-end effect). The total number of the fibres is controlled by a porosity.

The width and thickness of the fibre are about 11.1 μm (4 lattices) and 6.94 μm (2.5 lattices). The basis weight of the sheets is $45.6\,g\,m^{-2}$. The integers 0 and 1 are used to denote the void nodes and solid (fibre) nodes. To guarantee that the lattice Boltzmann equation is a faithful picture of the Navier–Stokes equations at low frequency and long-wavelength limits, we need to keep the size of the narrowest pore larger than four lattice units [21]. Therefore, any pore whose size is equal to or less than 3 units (8.33 μm) was artificially filled with solid nodes through a computer program. This limit of the resolution of the simulation can be improved by increasing the computer capacity, as will be discussed later. To model how the z-directional fibre orientation affects the transverse and in-plane permeabilities, we set $\omega = 0°$, 4.5°, 9°, 13.5° and 27° with a constant porosity of 0.706, for all five cases. The maximum polar angle, ω, larger than 27° may be rarely found in real paper [25]. A three-dimensional picture of the random fibre network structure constructed for the case of $\omega = 13.5°$ is shown Fig. 2.

The average density of particles and kinematic viscosity expressed in the natural unit are the same as those used for the Poiseuille flow examined earlier. To relate the dimensionless variables in the simulation to real physical quantities, the density of air, $1.2\,kg\,m^{-3}$,

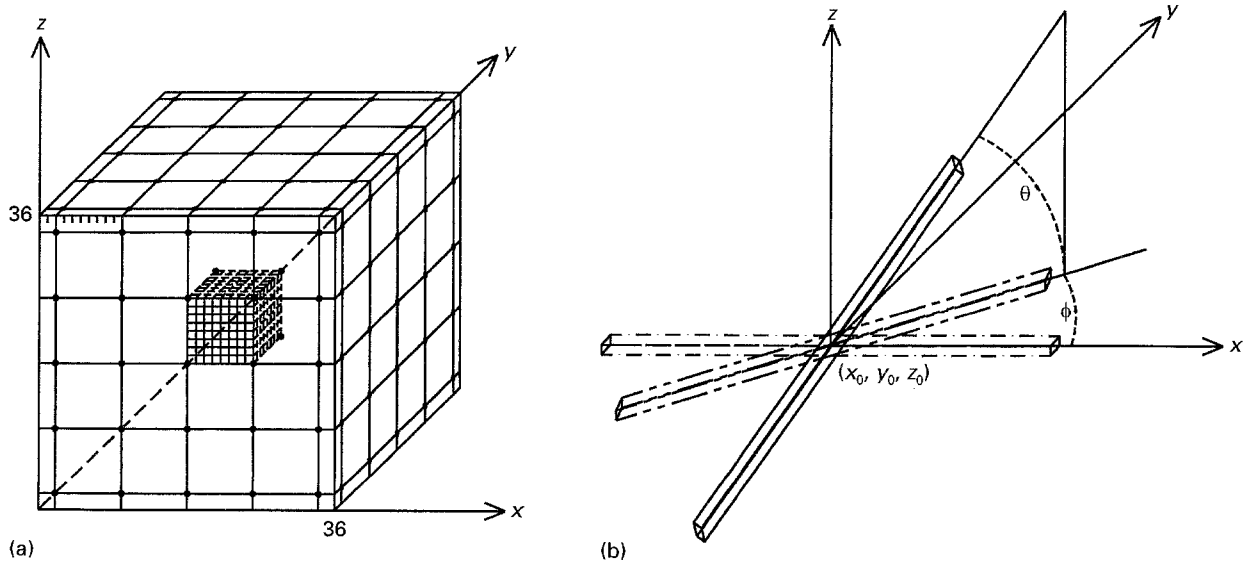

Figure 1(a) The simulation box. The simulation box was divided into 36 unit boxes. The sub-unit box contains 8 unit boxes. (b) Construction of fibre network. The initial position of a fibre is indicated by the broken lines. ϕ the angle between the x-axis and the normal projection of the fibre axis on to the x–y plane. θ, the angle between the fibre axis and the projected line on the x–y plane.

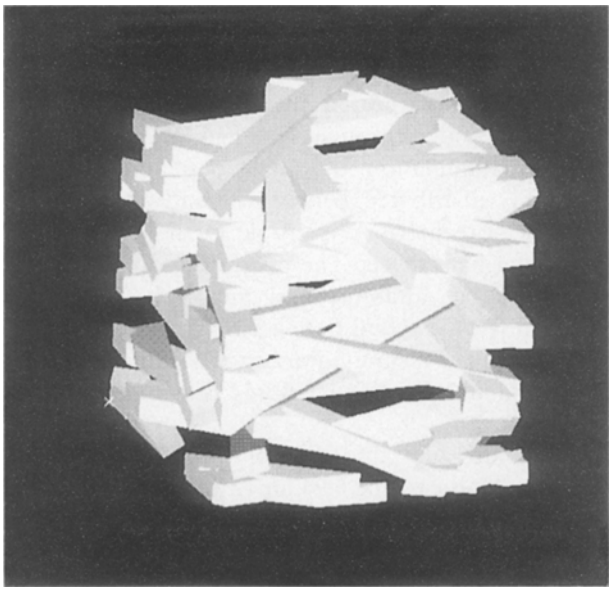

Figure 2 The interpenetrable three-dimensional fibre network ($\omega = 13.5°$ and porosity of 0.706).

and its kinematic viscosity, $1.5 \times 10^{-5}\ m^2\ s^{-1}$, are assumed. After dimensional analysis, we took $36\ m\ s^{-1}$ as the unit of velocity, 0.07716×10^{-6} s as the unit of time and 3.1462×10^{-18} kg as the unit of mass.

5. Permeability of the three-dimensional Fibre Network

Fig. 3 shows the mean velocity of air plotted against the pressure drop in the x-direction. The mean velocity is proportional to the pressure drop, indicating that the Darcy law holds within the pressure range tested. Fig. 4 shows the velocity field in the x–y plane at $z = 26$ when the pressure gradient, 336 kPa m^{-1}, is applied in the x-direction. The arrows represent the two-dimensional projection of the three-dimensional velocity vectors, and the hatched areas represent the section of the fibre network. Fig. 5 shows the velocity field in the y–z plane at $x = 10$ for the same numerical experiment. As expected, in Fig. 4 there is a systematic drift of air flow along the x direction, in which the pressure gradient is imposed, while in Fig. 5 there is no systematic drift in the section of the y–z plane. In Fig. 4 and 5, the velocity vector fields do not seem to reflect sensitively geometrical details of the solid (fibre) surface. The most of the flow seems to occur in relatively larger pores. Rothman observed in the simulation of flow through a two-dimensional porous medium that the majority of the flow follows just a few winding paths, while many areas are relatively stagnant [19]. This suggests that small pores and interstices do not proportionately contribute to permeability of the fibre network.

In Fig. 6, the transverse permeability, K_z, and the in-plane permeability, K_x, are plotted as functions of the maximum polar angle, ω, where the three-dimensional fibre orientation angle varies randomly between $-\omega$ and ω. With increasing three-dimensional fibre orientation, the transverse permeability increases and the in-plane permeability decreases. Both permeabilities

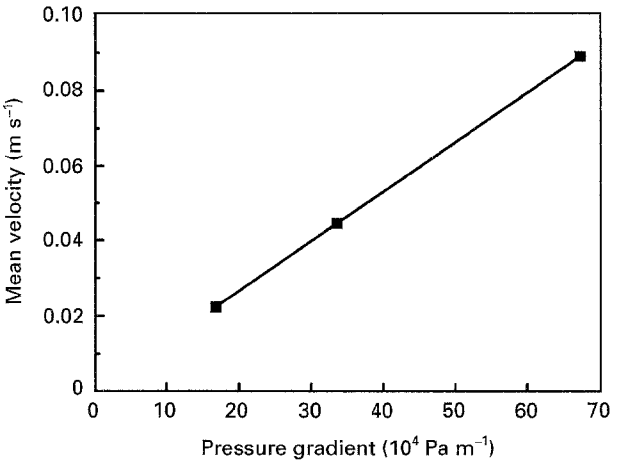

Figure 3 The relationship between mean velocity and pressure gradient for air flow in the x-direction ($\omega = 9°$).

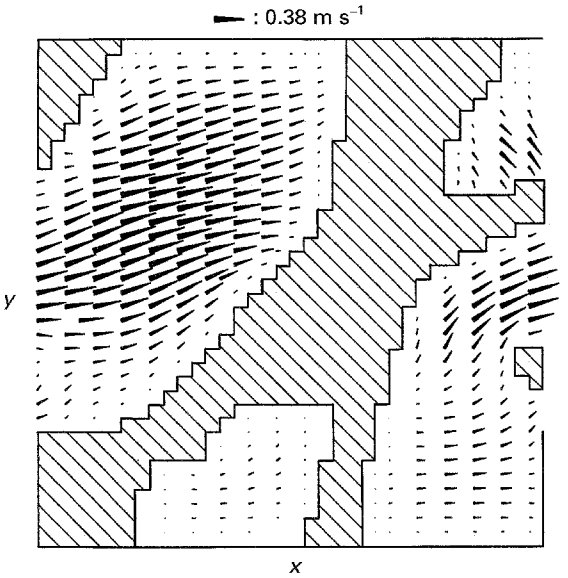

Figure 4 The velocity field in the x–y section at $z = 26$ ($\omega = 13.5°$). The section of the fibres is represented by hatched lines.

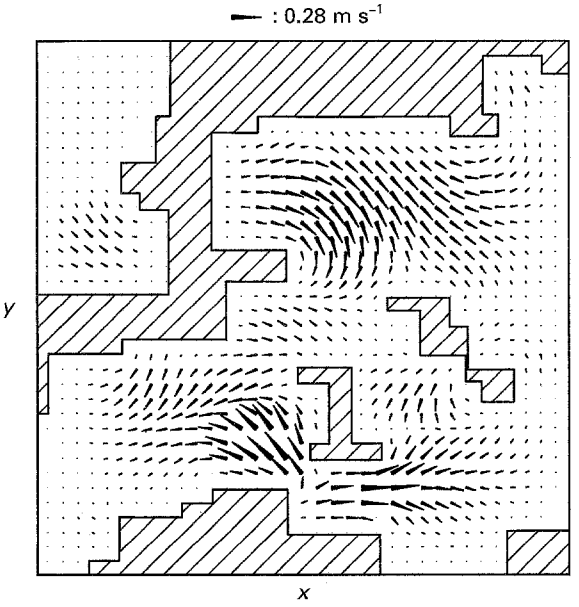

Figure 5 The velocity field in the y–z section at $x = 10$ ($\omega = 13.5°$).

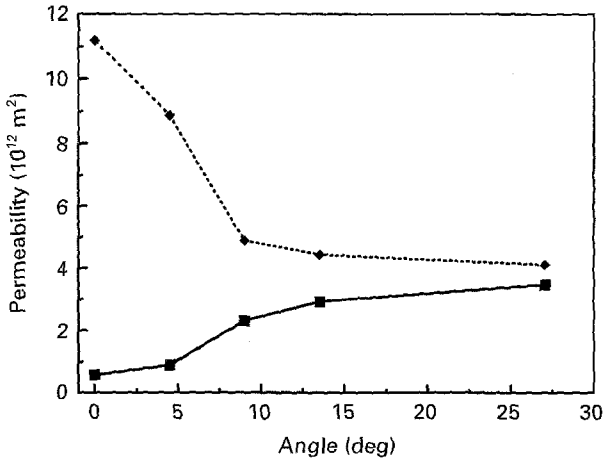

Figure 6 (■) Transverse permeability, K_z, and (◆) in-plane permeability, K_x, as a function of the polar angle of fibre segments.

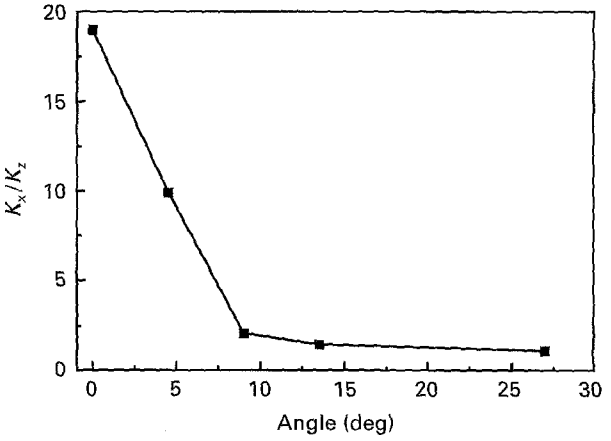

Figure 7 The ratio of K_x to K_z as a function of the polar angle of fibre segments.

show a dramatic change in the range of the maximum polar angle between 0° and 10°. It should be noted that the porosity was kept constant in this stimulation. Fig. 7 shows the ratio of K_x to K_z as a function of the polar angle. It is interesting to observe that permeability anisotropy is dramatically reduced with a relatively small increase of orientation of fibre segments in the z-direction. It is, therefore, clear that a correct description of the anisotropic permeability should include the three-dimensional fibre orientation.

Polat *et al.* experimentally determined air permeability in the z-direction (K_z) [1]. They found that K_z was 9.43×10^{-13} m^2 for handsheets of basis weight 25 g m^{-2} and porosity 0.684, and 2.62×10^{-13} m^2 for handsheets of basis weight 50 g m^{-2} and porosity 0.643. These results are remarkably comparable to the simulation results showing that $K_z = 8.95 \times 10^{-13}$ m^2 ($\omega = 4.5°$) and 5.9×10^{-13} m^2 ($\omega = 0°$) for the network of basis weight 45.6 g m^{-2} and porosity 0.706.

6. Conclusion

It was demonstrated that the lattice-gas Boltzmann model can be used to model successfully the paper structure–fluid interactions. We found that the in-plane permeability and the z-directional permeability are very sensitive to the orientation of fibre segments in the z-direction. At a constant porosity, the z-directional permeability increases and the in-plane permeability decreases with increasing the z-directional fibre orientation. This explains why the permeability varies considerably among different papers even at the same porosity, a typical question of papermakers.

Although the preliminary results presented in this paper showed the potential of the lattice-gas model for the simulation of various flow problems in porous media, some limitations of this method should be discussed. This work was conducted using a general-purpose workstation (HP 9000). The size of the simulation box was only $36 \times 36 \times 36$. Therefore, the resolution is not sufficient for detecting finer-scale flow; the flow through small pores of size less than 8 μm could not be detected. (This limitation may not be critical by considering the simulation results that fluid flow is not sensitive to smaller pores and interstices existing in the structure.) Another problem of the small simulation box is that there is a possible effect of boundary conditions. In particular, the type of the boundary condition used, such as solid-wall or periodic boundary conditions, could affect the calculated results of permeability. In addition, the small simulation box cannot contain a statistically representative number of fibres so that it is difficult to calculate effective properties, such as permeability, with sufficient statistical confidence. To overcome this difficulty, it would be most appropriate to use specialized, massively parallel, computers, as are currently being developed in some institutions [20].

Acknowledgements

The authors thank Professors J. Provan and L. Lassard, McGill University, for providing us with computer facilities, and Professor R. G. Cox and Dr R. H. Crotogino for reviewing the manuscript. One of the authors, D. Qi, acknowledges the Natural Sciences and Engineering Research Council of Canada for his Industrial Research Fellowship.

References

1. O. POLAT, R. H. CROTOGINO, A. R. P. VAN HEININGEN and W. J. M. DOUGLAS, *J. Pulp Paper Sci.* **19** (4) (1993) J137.
2. M. KATAJA, K. HILTUNEN and J. TIMONEN, *J. Phys. D. Appl. Phys.* **25** (1992) 1053.
3. L. WICKS, *Tappi* **65** (9) (1982) 73.
4. K. S. A. CHEN and L. E. SCRIVEN, *ibid.* **73** (1990) 151.
5. J. YI, T. AMARI and K. WATANABE, *Rep. Prog. Polym. Jpn* **32** (1989) 75.
6. J. BEAR, "Dynamics of Fluids in Porous Media" (Dover, New York, 1972).
7. U. FRISCH, B. HASSALACHERES and Y. POMEAU, *Phys. Rev. Lett.* **56** (1986) 1505.
8. U. FRISCH, D. D'HUMIERES, B. HASSLACHERES, P. LALLEMAND, Y. POMEAUS and J.-P. RIVET, *Complex Systems* **1** (1987) 649.
9. S. PRAGER, *Phys. Fluids* **4** (1961) 1477.
10. H. J. WEISSBERG and S. PRAGER, *ibid.* **13** (1970) 2958.
11. H. J. WEISSBERG, *Appl. Phys.* **34** (1963) 2636.

12. M. DOI, *J. Phys. Soc. Jpn* **40** (1976) 567.
13. S. TORQUATO, *Appl. Mech. Rev.* **44** (20) (1991) 37.
14. S. KIRKPATRICK, *Rev. Mod. Phys.* **45** (1973) 574.
15. M. SAHIMI, *Chem. Eng. Commun.* **64** (1984) 177.
16. D. D'HUMIERES, P. LALLEMAND and U. FRISCH, *Europhys. Lett.* **2** (1986) 291.
17. G. McNAMARA, and G. ZANETTI, *Phys. Rev. Lett.* **61** (1988) 2332.
18. H. CHEN, S. CHEN and W.H. MATTHAEUS, *Phys. Rev. A* **45** (1992) R5339.
19. D. H. ROTHMAN, *Geophys.* **53** (4) (1988) 509.
20. NATO Advanced Research Workshop, "Pattern Formation and Lattice-Gas Automata", p24, University of Waterloo, Waterloo, Canada, June 1993.
21. S. SUCCI, E. FOTI and F. HIGUERA, *Europhys. Lett.* **10**(5) (1989) 433.
22. M. HASUIKE, M. KAWASAKI and K. MURAKAMI, *J. Pulp Paper Sci.* **18**(3) (1992).
23. D. S. TSAI and W. STRIEDER, *Chem. Eng. Commun.* **40** (1986) 207.
24. S. TORQUATO and J. D. BEASLEY, *Int. J. Eng. Sci.* **24** (1986) 415.
25. H. R. CUSHING, PhD thesis, University of Minnesota (1991).

Received 20 February
and accepted 15 December 1995